Wood properties and chemical composition of the eccentric growth branch of Viburnum odoratissimum var. awabuki.

Yue Wang, Joseph Gril, Bruno Clair, Kazuya Minato, Junji Sugiyama

Wood properties and chemical composition of the eccentric growth branch of *Viburnum odoratissimum* var. *awabuki*

Yue Wang · Joseph Gril · Bruno Clair · Kazuya Minato · Junji Sugiyama

Abstract To clarify the wood properties and chemical composition of branches of *Viburnum odoratissimum* produced by unusual eccentric growth, we investigated growth strain (GS), basic density (D_b), microfibril angle (MFA), elastic moduli (E_L and E_L/D_b), creep deformation, cellulose crystalline features, and lignin structure in upper and lower sides of the branches, and considered the correlations among these factors. In most measuring positions, the distribution of GS showed that higher tensile GS was in the upper side and compressive GS was in the lower side of the branch, which combines GS features of reaction wood. However, the generation of GS in the lower side was different from that in compression wood, because E_L/D_b and MFA had a negative correlation. The creep compliance curves show that the upper-side wood had low rigidity and high viscosity, whereas the lower-side wood had large rigidity and low viscosity. Relative creep had a negative relation with MFA in the upper side, which is unusual. The cellulose crystalline features showed no obvious difference between both sides of the branch; however, the lignin with less β-*O*-4 proportion and less *S* units but more *G* units seemed to exist in the lower side because of a decreased syringyl/guaiacyl (*S*/*G*) molar ratio. This suggests that cell wall could be reinforced by lignin resulting in lower viscosity in the lower side of the branch. Additionally, the *S*/*G* ratio showed a relatively high correlation with GS in the lower side. These results suggest that lignin structure plays an important role in adapting to environmental changes during eccentric growth for *V. odoratissimum*.

Keywords Growth strain · Syringyl/guaiacyl ratio · Creep · Elastic modulus · Cellulose crystallinity

Y. Wang (✉) · J. Sugiyama
Laboratory of Biomass Morphogenesis and Information,
Research Institute for Sustainable Humanosphere,
Kyoto University, Uji, Kyoto 611-0011, Japan
e-mail: wangyuekyoto@rish.kyoto-u.ac.jp

J. Gril · B. Clair
Laboratoire de Mécanique et Génie Civil,
Université Montpellier 2, CNRS,
34095 Montpellier, France

K. Minato
Laboratory of Forest Resources Circulatory System,
Kyoto Prefectural University, Kyoto 606-8522, Japan

Introduction

In angiosperms, tension wood is generally induced on the upper side of inclined stems with eccentric growth, and has higher cellulose content than normal wood; in gymnosperms, compression wood is induced on the lower side of inclined stem with eccentric growth, and is characterized by higher lignin content (Onaka 1949; Timell 1986a, b, c). However, some special cases in angiosperms have occasionally been reported. For instance, *Buxus microphylla* Siebold & Zucc. shows pronounced growth on the lower side of inclined stems with large compressive stress. Its xylem has some anatomical features similar to those of compression wood (Yoshizawa et al. 1993), and the chemical structure of lignin shows a progressive grading from normal wood to reaction wood (Baillères et al. 1997). Similarly, growth eccentricity of *Pseudowintera colorata* (Raoul) Dandy occurs on the lower side of the inclined branches and the lower-side tracheids have a large microfibril angle (MFA) (Kucera and Philipson 1977, 1978; Meylan 1981). Regardless of reaction wood or special

cases, wood properties are closely related to chemical composition of wood.

We recently found that inclined branches of *Viburnum odoratissimum* var. *awabuki* (K. Koch) Zabel also have pronounced growth on the lower side (Fig. 1). Compared with *B. microphylla* and *P. colorata*, the anatomy of the branches of *V. odoratissimum* does not obviously differ between the upper and lower sides: the cell wall lacks gelatinous fiber and MFAs show no great differences. Uniquely, a relatively larger growth strain (GS) is commonly observed on the upper side opposite to the eccentric growth side. These results show that the branch of *V. odoratissimum* forms neither tension wood nor compression wood (Wang et al. 2009). Meanwhile, these results take some questions. For example, how does the branch keep a stably biomechanical situation, and why does eccentric growth occur in the lower side of branch even though *V. odoratissimum* is angiosperm.

In this study, we focused on understanding the abnormal biomechanics of branches exhibiting unusual eccentric growth. The wood properties, such as basic density (D_b), the elastic modulus in the longitudinal direction (E_L), creep deformation, and chemical composition of the branch were investigated. First, we measured the released surface GS in seven branches from two *V. odoratissimum* trees, and examined some physical and mechanical properties (D_b, MFA, E_L, E_L/D_b, creep compliance) of the branch wood. Second, we examined the cellulose crystalline features using attenuated total reflection infrared spectroscopy and X-ray diffraction (XRD) methods, and then analyzed the composition of guaiacyl unit (vanillin) and syringyl unit products comprising lignin by gas chromatography (GC). Finally, the relationship between wood properties and chemical composition in the branches was considered. Correlations among these factors would be advantageous to understand the biomechanics of branches.

Materials and methods

Plant material

GS of a *V. odoratissimum* tree (I) was measured in a previous study (Wang et al. 2009). Materials from this tree were used for chemical analysis. Two more 12-year-old *V. odoratissimum* trees (II and III) growing in Uji campus (130°82′E, 34°81′N–130°80′E, 34°81′N), Kyoto University, Japan were studied. The seven branches were 210–250 cm in length, and were inclined at angles between 50° and 60° from the vertical (the angle of branch no. 1 of tree III was 80°). After GS measurement, mechanical and chemical experiments were performed.

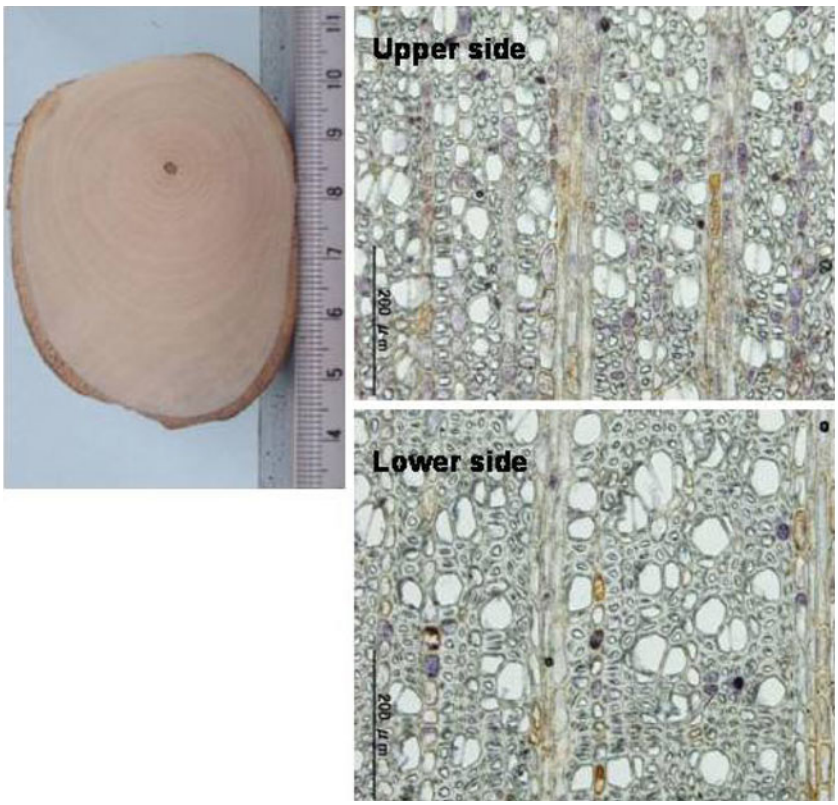

Fig. 1 Macro photo of the branch no. 3B of tree I and the cross sections stained with the mixed solution of zinc chloride and iodine. There is no G-layer in either side

Growth strain measurement

For trees II and III, GSs in two measuring positions (A and B) of seven branches were measured using a direct method in December 2008. The selection of measuring points was as described in a previous study (Wang et al. 2009). The direct method means that no twigs and branches were cut from the trees; after removing the bark at the measuring position, GS (ε_r) of the branch was directly measured using electrical resistance strain gauges by cutting grooves in the standing trees. The value of ε_r ($\varepsilon_r = \delta\varepsilon_r$) including the influence of self-loading is equal to the strain increment at stress release. Theoretically, values of ε_r obtained from both the direct and cumulative methods (Yoshida and Okuyama 2002; Wang et al. 2009) approach the real growth stress of the standing tree (Yamamoto et al. 1989; Jullien and Gril 2008).

Creep experiment, microfibril angle, and density

The branches of trees II and III were cut, and samples [$25(L) \times 2(T) \times 1(R)$ mm^3] at the mid-point of measuring positions A and B were cut from relatively new xylem of the upper and lower sides for corresponding to the results of released surface GS (Fig. 2). These samples were kept in water as green wood. The creep deformation of each green wood was tested using the cantilever condition for 5.7 h. The load was 0.45 N, well within the proportional limits, and the span was 20 mm. E_L and creep compliance were calculated. MFAs of the air-dried samples [$20(L) \times 2(T) \times 1(R)$ mm^3] were measured using an XRD method. Experiments were performed on a 4-circle diffractometer (Oxford Diffraction Gemini S) equipped with a 1,024 × 1,024 CCD camera. CuKα radiation was generated by an X-ray generator operating at 50 kV, 25 mA. Diffraction patterns were integrated between $2\theta = 21.5$ and 23.5 along the whole 360 azimuthal interval to plot the intensity diagram of the (200) plane. The average MFA of each sample was estimated using the method proposed by Cave (1966). The T parameter was measured as the half distance between intersections of tangents at inflexion points with the baseline. Finally, the D_b of the sample was expressed on the basis of the oven-dried weight and the swollen volume, and specific Young's modulus (E_L/D_b) was calculated.

Wood powder for chemical analysis

The wood chips of tree I were cut from two measuring positions of four branches, and then wood powder was prepared for chemical component analysis. The samples of trees II and III were cut from the same sample blocks which provided the samples for wood property experiments (Fig. 2). The wood powder was extracted with hot water at 60°C for 4 h, and successively extracted with benzene–ethanol (1/1, v/v) for 6 h.

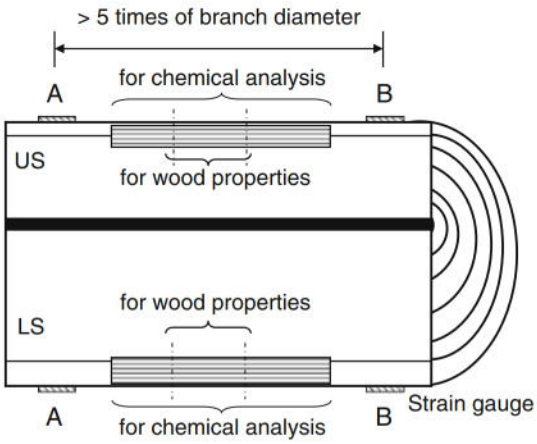

Fig. 2 Sample preparation. The samples for wood property experiments and chemical analysis were cut from relatively new xylem (*US* upper side, *LS* lower side)

Attenuated total reflection infrared spectroscopy and X-ray diffraction

Smooth radial-section samples were analyzed using a Spectrum One (PerkinElmer Co.) with ATR model. The angle of incidence was 45°. Attenuated total reflection infrared spectroscopy (ATR-FTIR) spectra were recorded between 4,000 and 400 cm^{-1} at a 4 cm^{-1} resolution.

The crystallinity index and crystallite width of cellulose in the wood samples [$5(T) \times 1(R) \times 15(L)$ mm^3] were measured using the XRD method. XRD was performed using a Rigaku X-ray diffractometer (UltraX 18HF), with CuKα radiation ($\lambda = 0.15418$ nm), operated at 40 kV, 300 mA and $2\theta = 5°$–40°. The crystallinity index was determined from the ratio of the separated crystalline peak area to the total reflection area including the background. The apparent crystallite width in the direction perpendicular to the 200 crystal plane was calculated using the Scherrer's equation (Cutter and Murphey 1972) as follows:

$$L = 0.9\lambda/H\cos\theta,$$

where λ is X-ray wavelength, H is the full-width at half-maximum at the radian, and θ is the Bragg angle. The Scherrer's equation theoretically applies to a perfect crystal. In reality, the peak broadening, quantified by parameter H, is affected by other factors than just the crystal size. Several studies (Burghammer et al. 2003; Kennedy et al. 2007) show that the Scherrer's equation is affected by the disorder within the crystal so it will be preferred to talk about apparent crystal size.

Klason lignin

The wood powder (0.5 g) was hydrolyzed at 20°C with 72% sulfuric acid (10 ml) for 4 h. The solute was diluted with distilled water until the sulfuric acid concentration was 3% and then boiled for 4 h. After rinsing and filtration, the oven-dried weight of Klason lignin was measured.

Nitrobenzene oxidation and acetylation

The extractives-free wood powder (100 mg) was mixed with 2 M sodium hydroxide (4 ml) and nitrobenzene (0.24 ml), and heated at 170°C for 2 h. After cooling, 2 ml of 5-iodovanillin-dioxane (4.19 mg/ml dioxane solution, internal standard) was added to the mixture. The mixture reaction solution was filtered and cleaned with 0.1 M sodium hydroxide, and pH of the rinsing solution was adjusted to 2–3 with 2 M hydrochloric acid. The acid aqueous solution was extracted with ethyl acetate and washed with saturated sodium chloride solution. The extract solution was successively dried with anhydrous sodium sulfate and the solvent was evaporated off under vacuum.

The dried 16 nitrobenzene oxidation samples from three trees were dissolved in acetic anhydride (0.5 ml) and pyridine (0.5 ml), and placed at 25°C for 24 h. Then the solvent of the mixture solution was evaporated off with ethanol under vacuum. The evaporated sample was dissolved in acetone (1 ml), and the solution (1 μl) was used to analyze lignin structure by GC measurement.

Gas chromatography

The product mixture was analyzed by GC–FID (GC-2014, Shimadzu) equipped with a SP-2330 capillary column (25 m × 0.25 mm, 0.25 μm film thickness). The GC conditions were as follows: injector 250°C, detector 270°C, column 230°C, and temperature program 5°C/min. The carrier gas was helium delivered at 30 ml/min. The correlation coefficients of the standard curves for *p*-hydroxybenzaldehyde, vanillin, and syringaldehyde were 0.9871, 0.9939, and 0.9964, respectively. The ratio of syringyl unit to guaiacyl unit (*S*/*G*) was calculated from the peak areas assigned to syringyl and vanillin type phenols.

Results and discussion

Growth strain of branches

Table 1 shows growth eccentricity and GSs of the branches of trees II and III. Growth eccentricity was found on the lower side of all branches except for 1B of tree II. The distribution of GS showed two patterns. One is tensile stress in the upper side and compressive stress in the lower side (the main pattern in trees II and III); the other is relatively higher tensile stress in the upper side and slight tensile stress in the lower side, like in the case of tension wood occurrence but with smaller GS levels (the main pattern in tree I). Although the E_L (see Table 2) of the lower side was slightly larger than that of the upper side ($P < 0.1$) except for tree II-3 and tree III-3, we could calculate that the growth stress in the upper side was greater than that in the lower side. This confirms that in contrast to the most usual pattern in angiosperm species, there was not a larger growth stress in the eccentric growth side of the stem.

According to the above results, we found that the eccentric growth in the lower side of the branch was a normal growth pattern for *V. odoratissimum* tree. The distribution of GS in the branch depended on the individual tree, but was in all cases characterized by a positive difference between the upper and lower sides to fulfill the

Table 1 Growth strains in the branches of trees II and III

Branch no.	R_1 (mm)	R_2 (mm)	Growth strain (μm/m)	
	Upper radius	Lower radius	Upper	Lower
Tree I				
1A	17	22	−205	16
1B	15	18	−706	433
2A	14	50	−191	−326
2B	10	20	−494	23
3A	22	55	−669	−53
3B	24	45	−553	−57
4A	25	55	−545	−212
4B	25	51	−520	−152
Tree II				
1A	11	31	−445	181
1B	15	15	−304	345
2A	12	21	−236	474
2B	12	16	−329	100
3A	11	30	−41	220
3B	18	24	−848	35
Tree III				
1A	12	36	−1,395	−91
1B	18	24	−357	−141
2A	8	15	−471	373
2B	9	12	−466	323
3A	14	28	−602	200
3B	12	19	−648	329
4A	12	18	−287	279
4B	12	14	−430	392

The data of tree I is from the previous study (Wang et al. 2009)

Table 2 Basic density, microfibril angle (MFA), elastic modulus in longitudinal direction (E_L), and specific modulus (E_L/D_b) of the branches

Branch no.	Basic density (g/mm^3)		MFA by XRD (°)		E_L (GPa)		E_L/D_b (GPa mm^3/g)	
	Upper	Lower	Upper	Lower	Upper	Lower	Upper	Lower
Tree II								
1	0.51	0.57	21.5	17.8	4.69	9.94	9.20	17.4
2	0.48	0.51	19.6	17.9	6.25	8.57	13.0	16.8
3	0.52	0.59	23.4	22.3	6.06	5.80	11.7	9.83
Tree III								
1	0.52	0.58	19.2	20.3	5.91	7.51	11.4	13.0
2	0.47	0.51	16.5	17.9	6.18	7.50	13.1	14.7
3	0.48	0.53	15.5	18.8	6.28	6.16	13.1	11.6
4	0.51	0.48	17.7	20.4	4.63	5.05	9.08	10.5

biomechanical requirements. This suggests that the mechanism responsible for eccentric growth of branch in *V. odoratissimum* trees is different from that for eccentric growth of branch in reaction wood of usual angiosperms species.

Physical and mechanical properties of branch wood

The D_b, MFA, E_L, and E_L/D_b of the branch wood in trees II and III are shown in Table 2. Because the lower-side wood had a large basic density, except for tree III-4, that can induce an increased elastic modulus of wood, the effect of density on E_L is shown in Fig. 3. We found that there was not a distinct relationship between both factors. Moreover, Fig. 4 shows the relationships between E_L/D_b (relating to the mean modulus), E_L (including the effect of cell-wall thickness) and MFA. In this case, there was no great difference in two relationships because the range of density was small. This also proves that the mechanical property of branch wood is not influenced by density. Meanwhile, the relationship between MFA and E_L/D_b was different in trees II and III: a clearly negative correlation in tree II ($R^2 = 0.75$), whereas a weak correlation in tree III ($R^2 = 0.09$), which may be due to branch architecture of individual tree. However, for trees II and III, the E_L/D_b of the lower side of the branch has a negative relation with MFA ($R^2 = 0.71$). This means that the generation of compressive GS in lower side is different from compression wood, because compression wood had a low E_L/D_b that obliges the tree to be denser in order to compensate for the lower cell-wall modulus resulting from high MFA.

Then, we investigated the viscoelastic property of the branch wood at green condition. Figure 5 shows the creep curves of green wood cut from the upper and lower sides of the branches. The creep compliance (J_t) of most upper-side samples was larger than that of the lower-side samples, suggesting that the upper-side sample had lower rigidity and higher viscosity. Higher creep is usually related to

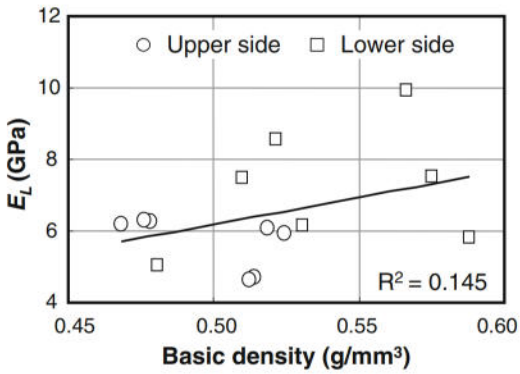

Fig. 3 Relationship between the basic density and E_L in the green branch wood

higher MFA. However, in Fig. 6, effect of MFA on relative creep ($J_{10,000}/J_{10} - 1$) showed a unique result, that is, there is a negative relationship between both factors in the upper side, which is in contradiction with expectation.

After considering GS and the wood properties of the branch, we found that the branch of *V. odoratissimum* has some features similar to reaction wood. The branch showed a distribution of GS similar either to tension wood (larger tensile growth stress in the upper side), or to compression wood (compressive growth stress in the lower side). Eccentric growth did not occur in the upper side, where no anatomical feature (for example, G-layer) of tension wood was visible. Although no particular anatomical feature was observed on the lower side either, from a biomechanical viewpoint of the generation of compression stress, in the case of the GS pattern (dominant in trees II and III), is consistent with the direction of eccentric growth and both are typical features of compression wood of gymnosperms, but a much lower specific modulus (E_L/D_b) associated with a higher MFA. The higher rigidity and lower fluidity of the lower side acts also consistently with the biomechanical requirement of the branch, which would not be necessarily

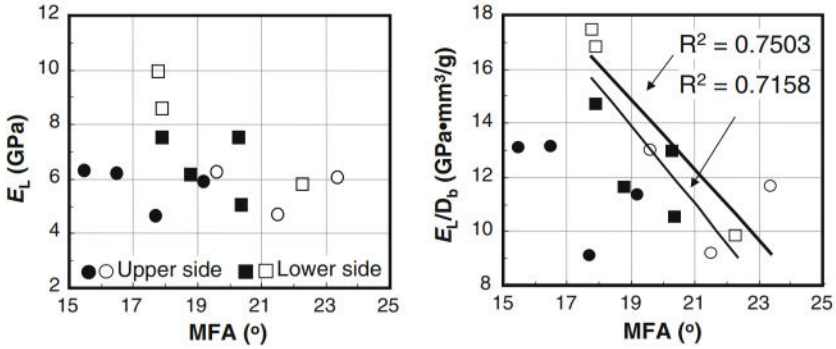

Fig. 4 Relationships between E_L, E_L/D_b and MFA in trees II (*hollow mark*) and III (*solid mark*)

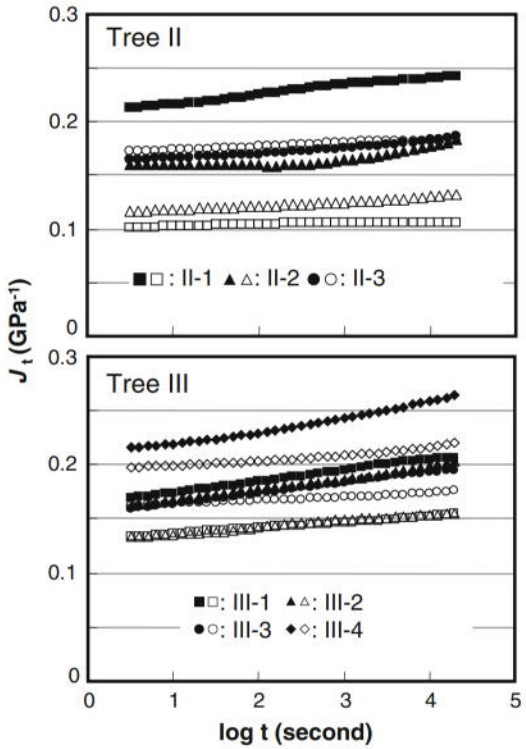

Fig. 5 The creep compliance curves of green wood cut from the upper and lower sides of branches (*solid mark* the upper side; *hollow mark* the lower side)

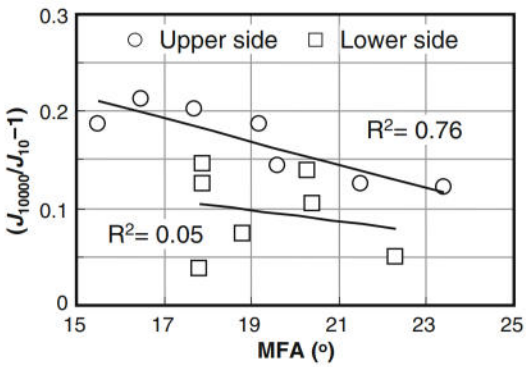

Fig. 6 Relationship between the relative creep ($J_{10,000}/J_{10}-$ 1) and MFA in trees

characterized by a higher density like in the case of compression wood. Although negative GSs were measured, especially in tree I, their level was not sufficient to indicate compression wood. Moreover, the MFA values and their negative correlation with creep show that this branch wood does not correspond to usual trend of normal wood versus reaction wood. Therefore, it is necessary to consider the influences of chemical composition and matrix structure of cell wall on viscoelastic property of the branch.

Cellulose crystalline features in branches

The ATR-FTIR spectra of branch (tree I-3B) are shown in Fig. 7. Peaks of the spectra showed the typical characteristic of hardwood. Peak heights of 1,734 cm^{-1} for unconjugated C=O in xylans and 1,505 cm^{-1} for aromatic skeletons in lignin (Pandey 1999; Pandey and Pitman 2003) were not obviously different between both sides of the branch. The same result was also obtained from other branches.

Table 3 shows the crystallinity index and the apparent crystallite width in the branches exhibiting unusual eccentric growth. The development of crystallinity in the lower side due to eccentric growth was expected because crystallinity influences the mechanical properties of the cellulose fiber (Lee 1961). In fact, although the crystallinity index in the lower side seems to be less than that in the upper side for most of the samples, there was no significant

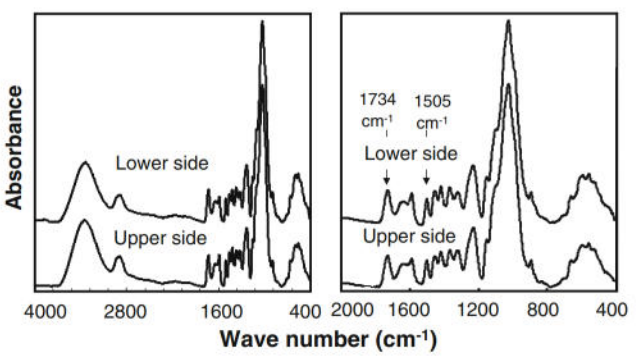

Fig. 7 ATR-FTIR spectra of the branch (tree I-3B) for *V. odoratissimum*

difference, while the apparent crystallite width had no change in both sides of the branches. Therefore, although the lower side of the branch had a larger E_L in *V. odoratissimum*, this property is not explained by cellulose crystallinity.

In addition, Washusen and Evans (2001) reported that tension wood has wider crystallites than normal wood in *Eucalyptus globulus*. The apparent crystallite width was less in compression wood than in the opposite wood of Japanese red pine (Tanaka et al. 1981). Thus, it is generally believed that crystallinity changes with eccentric growth. Compared with these cases, in *V. odoratissimum*, the lower side of the branch, which exhibits eccentric growth, did not obviously have different crystalline features, confirming that growth eccentricity in *V. odoratissimum* is not associated with reaction wood production.

Lignin structure in branches

Lignin is an important chemical composition of wood. Its content is 25–35% in softwood and 17–25% in hardwood (Tsoumis 1991). The lignin content in the branches of *V. odoratissimum* is shown in Table 3. The Klason lignin content was about 20–30% in both sides, depending on the individual tree, exhibiting a good lignification. Moreover, Klason lignin had a slight but significant distribution pattern in the branch. That is, the Klason lignin content in the lower side was higher than that in the upper side of the branch except for the branch no. 1 of tree III ($P < 0.05$). This distribution pattern also suggests that the upper side should have higher content of cellulose. Although this trend is consistent with what is observed in the case of reaction wood occurrence, either tension wood in the upper side or compression wood in the lower side, when the relationship between the lignin content and GS was considered (Fig. 8), a relatively weak correlation between both factors in the lower side was observed. In fact, the branches did not display a larger compressive stress in the lower side or a remarkable tensile stress in the upper side as in reaction wood.

Furthermore, lignin is described as a three-dimensional structure formed by phenylpropane units. In general, softwood is rich in guaiacyl (*G*) units while guaiacyl and syringyl (*S*) units are present in hardwood. The *p*-hydroxyphenyl (*H*) unit is typical of compression wood lignin (Timell 1986a). Yoshida et al. (2002a) reported that the *S*/*G* ratio increases with tensile released strain in yellow poplar that does not form G-layer. Similar results were obtained in black locust (Yoshida et al. 2002b) and eucalyptus (Baillères et al. 1995; Aoyama et al. 2001). To investigate the effect of *S*/*G* ratio on GS in *V. odoratissimum*, the lignin structure was analyzed using GC measurement.

The relative molar distributions of *S*/*G* in the upper and lower sides of the branches are summarized in Table 3. Although eccentric growth occurs on the lower side of the branch, the H unit was not detected in either side, implying that growth eccentricity in *V. odoratissimum* is different from that in compression wood and *Buxus* wood (this result should be also checked using thioacidolysis). *S* and *G* units were widely present in the branches, indicating that relatively reactive ether bond (*β*-*O*-4) linked *G* and *S* units is a

Table 3 The factors of chemical structures in the branches of *V. odoratissimum*

Branch no.	Crystallinity index (%)		Crystallite width (nm)		Klason lignin content (%)		Total yield of products (S + G, μmol/g of Klason lignin)		*S*/*G* ratio	
	Upper	Lower	Upper	Lower	Upper	Lower	Upper	Lower	Upper	Lower
Tree I										
1A	43.0	36.1	4.0	4.0	26.5	27.8	3,487	3,366	2.24	1.41
1B	35.7	35.3	4.0	4.0	25.3	26.9	3,956	2,340	1.86	1.63
2A	36.7	36.1	4.0	4.0	27.1	28.8	2,291	1,701	1.78	1.27
2B	35.0	38.1	4.0	4.0	26.7	28.3	2,035	2,230	1.94	1.56
3A	32.9	33.9	4.0	4.0	27.2	28.2	2,610	2,062	1.94	1.27
3B	34.4	33.1	4.0	4.0	26.5	28.9	3,593	2,353	2.03	1.44
4A	32.1	36.6	4.0	4.0	27.7	29.1	3,517	2,298	1.50	1.06
4B	36.1	34.7	4.0	4.0	27.8	29.9	3,226	3,191	1.94	1.13
Tree II										
1	35.2	32.4	4.0	4.0	21.0	23.8	2,566	1,963	2.33	1.30
3	35.3	31.9	4.0	4.0	19.9	21.4	2,758	1,988	2.57	1.49
Tree III										
1	34.7	31.9	4.0	4.0	25.3	25.1	1,674	1,407	2.57	1.33
3	33.1	31.0	4.0	4.0	25.4	26.0	1,654	1,438	2.03	1.56

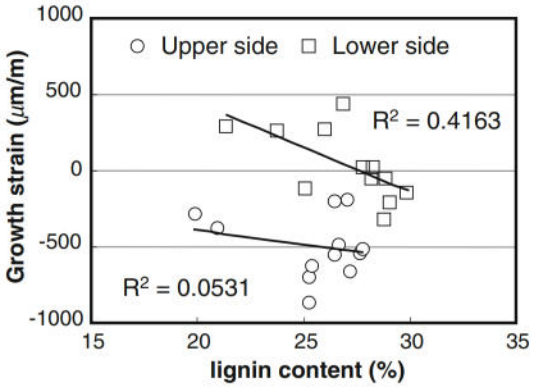

Fig. 8 Relationship between lignin content and growth strain. GS values of tree I are from the previous study (Wang et al. 2009). The GSs of the branch of trees II and III are average values of two measuring positions

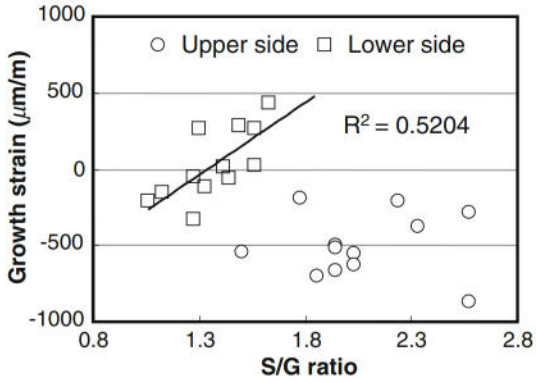

Fig. 9 Relationship between *S/G* ratio and growth strain. GS values of tree I are from the previous study (Wang et al. 2009). The GSs of trees II and III are average values of two measuring positions of each branch

structural feature in *V. odoratissimum* common to angiosperms. By comparing the total yield in both sides, we observed that the yield of products in the lower side was less than that in the upper side except for tree I-2B ($P < 0.05$). This result suggests that the *β-O*-4 structure, which is the noncondensed-type, is less common in the lower side of the branch. The varying distribution of *S/G* shows the following trend: *S* units decreased and *G* units increased in the lower side of the branch, that is, the *S/G* ratio in the eccentric growth side (lower side) was lower than that in the normal growth side (upper side).

These results suggest that the quality of lignin in the branch is different due to the proportion of *β-O*-4 and *S/G* ratio. Less *β-O*-4 proportion, and less *S* units but more *G* units seem to exist in the lignin of the lower side, whereas more *β-O*-4 proportion, and more *S* units but less *G* units seem to be present in the lignin of the upper side of the branch, suggesting that cell wall is reinforced by different type of lignin from that of the upper side during lignification in the lower side because lignin serves as glue to stiffen the matrix structure of cell wall. Hence, the mechanical properties of the branch seem to be controlled by the lignin structure. Particularly, regard as a compressive GS in the lower side, the lower *S/G* ratio can replace a low E_L/D_b of compression wood, and is more efficient. Therefore, the lower side of the branch had higher rigidity and lower viscosity to sustain downward bending due to the gravity.

Then, the effect of *S/G* ratio on the GS of the branches was considered. A general trend is found in Fig. 9: higher *S/G* ratio with tensile GS and lower *S/G* ratio with mostly compressive GS. This is consistent with usual trend between tension wood and normal wood (Baillères et al. 1995; Aoyama et al. 2001; Yoshida et al. 2002a). Furthermore, we found that GS decreased with a decreased *S/G* ratio in the lower side of the branch. There was a relatively high correlation ($R^2 = 0.52$) between GS and *S/G* ratio in the lower side. It seems that the matrix of cell wall reinforced by the lignin with less *β-O*-4 proportion and smaller *S/G* ratio resists growth stress in the lower side of the branch. In the upper side, the lignin with more *β-O*-4 proportion and larger *S/G* ratio was more common so that the amount of GS was not restricted by lignin structure. Thus, for most of the branches in *V. odoratissimum*, a larger GS occurs in the upper side opposite to the eccentric growth side. These results indicate that the rigid lower side would restrain the downward deformation of the upper side of the branch.

Conclusion

Although eccentric growth is found in the lower side of the branches of *V. odoratissimum*, the distribution of GS combined the characters of tension wood (tensile GS in the upper side) and compression wood (compressive GS in the lower side) without any anatomical features of reaction wood. However, the lower-side wood has not a lower E_L/D_b to compensate for the low cell-wall modulus resulting from high MFA, like in the case of compression wood. The upper-side wood had low rigidity and high viscosity, whereas the lower-side wood had large rigidity and low viscosity. Relative creep of the upper-side wood had a negative relation with MFA, which is in contradiction with usual belief. The cellulose crystalline features in the lower side were not significantly different from those in the upper side. On the other hand, the lignin structure showed a clear distinction between both sides of the branch, that is, *S/G* ratio decreased in the lower side, suggesting that the lignin with less *β-O*-4 proportion, and less *S* units but more *G* units exists in the lower side, and greatly influenced the GS of the branch. It seems that the matrix structure of cell wall of the

lower side become stiffer due to an increased *S*/*G* ratio. Therefore, the chemical properties of lignin may control the amount of GS and the mechanical properties of the branches. These results also indicate that *V. odoratissimum* has different growth biomechanics to other woody plants in order to adapt to changes in the environment.

Acknowledgments This study was supported by Grant-in-Aid for foreign research fellows (No. 20.08105) provided by the Japan Society for the Promotion of Science. The authors thank members of the Laboratory of Forest Resources Circulatory System, Kyoto Prefectural University, Japan for assistance with GC measurement.

References

Aoyama W, Matsumura A, Tsutsumi Y, Nishida T (2001) Lignification and peroxidase in tension wood of *Eucalyptus viminalis* seedlings. J Wood Sci 47:419–424

Baillères H, Chanson B, Fournier M, Tollier MT, Monties B (1995) Structure, composition chimique et retraits de maturation du bois chez les clones d'Eucalyptus. Ann For Sci 52:157–172

Baillères H, Castan M, Monties B, Pollet B, Lapierre C (1997) Lignin structure in *Buxus sempervirens* reaction wood. Phytochemistry 44:35–39

Burghammer M, Műller M, Riekel C (2003) X-ray synchrotron radiation microdiffraction on fibrous biopolymers like cellulose and in particular spider silks. Recent Res Dev Macromol 7:103–125

Cave ID (1966) Theory of X-ray measurement of microfibril angle in wood. For Prod J 16:37–42

Cutter BE, Murphey WK (1972) X-ray measurement of crystallite size in wood. Wood Fiber 4:43–44

Jullien D, Gril J (2008) Growth strain assessment at the periphery of small-diameter trees using the two-grooves method: influence of operating parameters estimated by numerical simulations. Wood Sci Technol 42:551–565

Kennedy CJ, Cameron GJ, Šturcová A, Apperley DC, Altaner C, Wess TJ, Jarvis MC (2007) Microfibril diameter in celery collenchyma cellulose: X-ray scattering and NMR evidence. Cellulose 14:235–246

Kucera LJ, Philipson WR (1977) Growth eccentricity and reaction anatomy in branchwood of *Drimys winteri* and five native New Zealand tress. N Z J Bot 15:517–524

Kucera LJ, Philipson WR (1978) Growth eccentricity and reaction anatomy in branchwood of *Pseudowintera colorata*. Am J Bot 65:601–607

Lee CL (1961) Crystallinity of wood cellulose fiber. For Prod J 11:108–112

Meylan BA (1981) Reaction wood in *Pseudowintera colorata*—a vessel-less dicotyledon. Wood Sci Technol 15:81–92

Onaka F (1949) Studies on compression- and tension-wood. Wood Res 1:1–88 (in Japanese)

Pandey KK (1999) A study of chemical structure of soft and hardwood and wood polymers by FTIR spectroscopy. J Appl Polym Sci 71:1969–1975

Pandey KK, Pitman AJ (2003) FTIR studies of the changes in wood chemistry following decay by brown-rot and white-rot fungi. Int Biodeterior Biodegrad 52:151–160

Tanaka F, Koshijima T, Okamura K (1981) Characterization of cellulose in compression and opposite woods of a *Pinus densiflora* tree grown under the influence of strong wind. Wood Sci Technol 15:265–273

Timell TE (1986a) Compression wood in gymnosperms, vol 1. Springer, Berlin, pp 63–89

Timell TE (1986b) Compression wood in gymnosperms, vol 3. Springer, Berlin, pp 1757–1791

Timell TE (1986c) Compression wood in gymnosperms, vol 3. Springer, Berlin, pp 1799–1824

Tsoumis G (1991) Science and technology of wood: structure, properties, utilization. Van Nostrand Reinhold, New York, pp 88–91

Wang Y, Gril J, Sugiyama J (2009) Variation in xylem formation of *Viburnum odoratissimum* var. *awabuki*: growth strain and related anatomical features of branches exhibiting unusual eccentric growth. Tree Physiol 29:707–713

Washusen R, Evans R (2001) The association between cellulose crystallite width and tension wood occurrence in *Eucalyptus globulus*. IAWA J 33:235–243

Yamamoto H, Okuyama T, Iguchi M (1989) Measurement of growth stresses on the surface of a leaning stem. Mokuzai Gakkashi 35:595–601 (in Japanese)

Yoshida M, Okuyama T (2002) Techniques for measuring growth stress on the xylem surface using strain and dial gauges. Holzforschung 56:461–467

Yoshida M, Ohta H, Yamamoto H (2002a) Tensile growth stress and lignin distribution in the cell walls of yellow poplar, *Liriodendron tulipifera* Linn. Tree Struct Funct 16:457–464

Yoshida M, Ohta H, Yamamoto H (2002b) Tensile growth stress and lignin distribution in the cell walls of black locust (*Robinia pseudoacacia*). J Wood Sci 48:99–105

Yoshizawa N, Satoh M, Yokota S, Idei T (1993) Formation and structure of reaction wood in *Buxus microphylla* var. *insularis* Nakai. Wood Sci Technol 27:1–10